# Matching-pursuit/split-operator-Fourier-transform simulations of excited-state nonadiabatic quantum dynamics in pyrazine

Xin Chen and Victor S. Batista[a)]
*Department of Chemistry, Yale University, New Haven, Connecticut 06520-8107*

(Received 20 July 2006; accepted 25 August 2006; published online 28 September 2006)

A simple approach for numerically exact simulations of nonadiabatic quantum dynamics in multidimensional systems is introduced and applied to the description of the photoabsorption spectroscopy of pyrazine. The propagation scheme generalizes the recently developed matching-pursuit/split-operator-Fourier-transform (MP/SOFT) method [Y. Wu and V. S. Batista, J. Chem. Phys. **121**, 1676 (2004)] to simulations of nonadiabatic quantum dynamics. The time-evolution operator is applied, as defined by the Trotter expansion to second order accuracy, in dynamically adaptive coherent-state expansions. These representations are obtained by combining the matching-pursuit algorithm with a gradient-based optimization method. The accuracy and efficiency of the resulting computational approach are demonstrated in calculations of time-dependent survival amplitudes and photoabsorption cross sections, using a model Hamiltonian that allows for direct comparisons with benchmark calculations. Simulations in full-dimensional potential energy surfaces involve the propagation of a 24-dimensional wave packet to describe the $S_1/S_2$ interconversion of pyrazine after $S_0 \rightarrow S_2$ photoexcitation. The reported results show that the generalized MP/SOFT method is a practical and accurate approach to model nonadiabatic reaction dynamics in polyatomic systems. © *2006 American Institute of Physics*. [DOI: 10.1063/1.2356477]

## I. INTRODUCTION

Nonadiabatic quantum dynamics is a ubiquitous phenomenon common to a wide range of physical, chemical, and biological processes.[1,2] Within the context of photochemical reactions in polyatomic systems, ultrafast nonadiabatic dynamics often determines the underlying molecular relaxation after UV-visible photoexcitation. These processes produce broad and structureless photoabsorption spectra, masking the spectroscopic features that could provide a structural and dynamical description of the system at the molecular level. Therefore, rigorous interpretations of spectroscopy often require detailed investigation using computational methods where quantum effects are explicitly considered. This paper introduces one such method as a generalization of the recently developed matching-pursuit/split-operator-Fourier-transform (MP/SOFT) approach[3–8] and its first application to a realistic molecular problem, the $S_1/S_2$ interconversion dynamics of pyrazine after $S_0 \rightarrow S_2$ photoexcitation.

The photophysics of pyrazine provides a standard platform for studying the case of interest, ultrafast internal conversion responsible for a broadband photoabsorption spectrum with a rather diffuse superimposed structure. The underlying excited-state nonadiabatic dynamics, following $S_0 \rightarrow S_1(\pi,\pi^*)$, $S_2(n,\pi^*)$ photoexcitation, is also ideally suited to benchmark the capabilities of new theoretical methods, since it has been extensively investigated both experimentally[9,10] and theoretically.[11–17] *Ab initio* calculations have characterized the existence of a conical intersection between the $S_1$ and $S_2$ states, leading to ultrafast intramolecular energy transfer.[11] The experimental $S_2$ photoabsorption spectrum has been reproduced by using a four-mode model Hamiltonian, after convoluting the resulting spectrum with an experimental resolution function,[18] or explicitly including the effect of the remaining vibrational modes as a weakly coupled harmonic bath.[12] These two models have allowed for direct comparisons between benchmark calculations and state-of-the-art semiclassical and quantum mechanical methods, including the multiconfigurational time dependent Hartree (MCTDH) approach,[12] the Herman-Kluk semiclassical initial value representation (SC-IVR) method,[14] the multiple spawning quantum approach,[15] the time dependent Gauss-Hermite discrete value representation (TDGH-DVR) method,[16] and the coupled coherent-state (CCS) technique.[17] Here, the capabilities of the generalized MP/SOFT approach are evaluated as applied to the description of the photoabsorption spectroscopy of pyrazine.

Describing electronic nonadiabaticity in excited electronic states of polyatomic systems is a challenging problem. At the most fundamental level of theory, it requires solving the system of coupled differential equations defined by the multichannel time-dependent Schrödinger equation. This problem can be rigorously solved by applying numerically exact methods for wave-packet propagation,[19–31] for example, approaches based on the split-operator-Fourier-transform (SOFT) method,[32–34] the Chebyshev expansion,[35] and the short iterative Lanczos algorithms.[36] These rigorous approaches demand storage space and computational effort that scale exponentially with the number of coupled degrees of freedom in the system. Their applicability is therefore limited to rather small systems (e.g, molecular systems with less than three or four atoms). For this reason, studies of

[a)]Author to whom correspondence should be addressed. Electronic mail: victor.batista@yale.edu

 

nonadiabatic dynamics in polyatomic systems are usually based on approximate methods built around semiclassical and mixed quantum-classical treatments.[37–51] However practical, these popular approaches rely upon *ad hoc* approximations whose consequences are often difficult to quantify in applications to complex (i.e., nonintegrable) dynamics. It is, therefore, an important challenge to develop practical (yet rigorous) methods for validating approximate approaches as well as for providing new insights into the nature of quantum dynamics at the most fundamental level of theory.[3–8,12,14–17]

The recently developed MP/SOFT method[3–8] is a simple time-dependent propagation scheme for simulations of quantum processes in multidimensional systems. The approach is based on coherent-state expansions of the time-dependent wave packet generated according to the matching-pursuit algorithm.[52] These compact representations allow for the efficient propagation of multidimensional wave packets by analytically applying the time-evolution operator as defined by the Trotter expansion to second order accuracy. The method thus bypasses the exponential scaling problem of the standard grid-based SOFT approach,[32–34] a method that is usually limited by the capabilities of the fast-Fourier-transform (FFT) algorithm.[53] When compared to alternative time-dependent methods based on coherent-state expansions,[15,54–68] the MP/SOFT method is usually easier to implement since it has the advantage of avoiding the need of propagating time-dependent expansion coefficients, a task that would require solving a coupled system of differential equations. Furthermore, the MP/SOFT method overcomes the truncation problem (natural to propagation schemes where the basis set, or grid base, is defined *a priori*) by dynamically adapting the coherent-state expansion according to the desired propagation accuracy. As a technical matter, the MP/SOFT method also overcomes the usual numerical difficulties introduced by overcomplete basis sets,[23] simply by implementing the matching-pursuit successive orthogonal decomposition scheme to reduce the underlying redundancy of the overcomplete representation. The main drawback of the MP/SOFT method is that it requires generating a new coherent-state expansion for each propagation step. The underlying computational task, however, can be trivially parallelized. In applications to multidimensional problems, the resulting algorithm overcomes the otherwise limitations of memory/storage bandwidth in terms of readily available processing power.

The capabilities of the MP/SOFT method have been recently demonstrated in several simulations of adiabatic quantum dynamics, including tunneling in model systems with up to 20 coupled degrees of freedom[5] and the excited-state intramolecular proton transfer in 2-(2′-hydroxyphenyl)-oxazole as modeled by the propagation of a 35-dimensional wave packet.[8] The MP/SOFT approach has also been applied to the description of thermal-equilibrium density matrices, finite-temperature time-dependent expectation values, and time-correlation functions.[6] Furthermore, MP/SOFT has been applied to the description of nonadiabatic quantum dynamics in conjunction with a perturbational description of the nonadiabatic couplings.[7] However, there remains the nontrivial question as to whether the MP/SOFT method can be rigorously implemented to model nonadiabatic processes without relying on any perturbational approximation. This paper shows that indeed MP/SOFT can be effectively applied for rigorous simulations of nonadiabatic dynamics according to a numerically exact algorithm.

The paper is organized as follows. Section II describes the generalization of the MP/SOFT method to simulations of nonadiabatic quantum dynamics, the calculation of photoabsorption spectra, and the model Hamiltonian. An alternative implementation of the method is described in the Appendix, where both the diabatic propagation and the coupling between wave-packet components are combined in a single matching-pursuit expansion, rather than in separate propagation steps. Section III presents the results for the reduced four-mode model Hamiltonian of pyrazine and the comparison to the corresponding results obtained according to benchmark grid-based SOFT calculations. Furthermore, Sec. III presents full-dimensional simulations of $S_1/S_2$ internal conversion, as described by the nonadiabatic propagation of the 24-dimensional wave packet. Finally, Sec. IV summarizes and concludes.

## II. METHODOLOGY

### A. Generalized MP/SOFT method

The generalization of the MP/SOFT method, introduced in this paper, is based on the recursive application of the Trotter expansion to second order accuracy,

$$e^{-i\hat{H}2\tau} \approx e^{-i\hat{H}_0(\hat{\mathbf{x}})\tau} e^{-i\hat{V}_c 2\tau} e^{-i\hat{H}_0(\hat{\mathbf{x}})\tau}, \tag{1}$$

where $\tau$ is a sufficiently short time increment. To keep the notation as simple as possible, all expressions are written in atomic units, so $\hbar=1$.

The system evolves according to the Hamiltonian

$$\hat{H} = \hat{H}_0 + \hat{V}_c, \tag{2}$$

where

$$\hat{H}_0 = \frac{\hat{\mathbf{p}}^2}{2m} + \sum_{k=1}^{n} V_k(\mathbf{x})|k\rangle\langle k| \tag{3}$$

describes the propagation of individual wave-packet components evolving on the diabatic potential energy surfaces $V_k$. In addition,

$$\hat{V}_c = \sum_{k=1}^{n}\sum_{j\neq k}^{n} V_{kj}(\mathbf{x})|j\rangle\langle k| \tag{4}$$

represents the couplings between diabatic states. The parametrization of $\hat{H}_0$ and $\hat{V}_c$ is described in Sec. II C.

In order to analyze the nonadiabatic dynamics of pyrazine, after $S_0 \rightarrow S_2$ photoexcitation, we focus on the two-level ($n=2$) time-dependent wave packet,

$$|\Psi(\mathbf{x};t)\rangle = \varphi_1(\mathbf{x};t)|1\rangle + \varphi_2(\mathbf{x};t)|2\rangle, \tag{5}$$

where $\varphi_1(\mathbf{x};t)$ and $\varphi_2(\mathbf{x};t)$ are the nuclear wave-packet components associated with the $S_1$ and $S_2$ states $|1\rangle$ and $|2\rangle$, respectively.

The MP/SOFT implementation of Eq. (1), as applied to the propagation of the initial state introduced by Eq. (5), involves the following steps.

(I) Propagate $\varphi_1(\mathbf{x};t)$ and $\varphi_2(\mathbf{x};t)$ diabatically for time $\tau$,

$$\begin{pmatrix} \varphi_1'(\mathbf{x};t+\tau) \\ \varphi_2'(\mathbf{x};t+\tau) \end{pmatrix} = \begin{pmatrix} e^{-i[\hat{\mathbf{p}}^2/2m+V_1(\hat{\mathbf{x}})]\tau} & 0 \\ 0 & e^{-i[\hat{\mathbf{p}}^2/2m+V_2(\hat{\mathbf{x}})]\tau} \end{pmatrix} \times \begin{pmatrix} \varphi_1(\mathbf{x};t) \\ \varphi_2(\mathbf{x};t) \end{pmatrix}. \tag{6}$$

(II) Couple the two wave-packet components $\varphi_1'(\mathbf{x};t+\tau)$ and $\varphi_2'(\mathbf{x};t+\tau)$,

$$\begin{pmatrix} \varphi_1''(\mathbf{x};t+\tau) \\ \varphi_2''(\mathbf{x};t+\tau) \end{pmatrix} = \mathbf{M} \begin{pmatrix} \varphi_1'(\mathbf{x};t+\tau) \\ \varphi_2'(\mathbf{x};t+\tau) \end{pmatrix}, \tag{7}$$

with

$$\mathbf{M} \equiv \begin{pmatrix} \cos(2V_c(\hat{\mathbf{x}})\tau) & -i\sin(2V_c(\hat{\mathbf{x}})\tau) \\ -i\sin(2V_c(\hat{\mathbf{x}})\tau) & \cos(2V_c(\hat{\mathbf{x}})\tau) \end{pmatrix}. \tag{8}$$

(III) Propagate $\varphi_1''(\mathbf{x};t+\tau)$ and $\varphi_2''(\mathbf{x};t+\tau)$ diabatically for time $\tau$,

$$\begin{pmatrix} \varphi_1(\mathbf{x};t+2\tau) \\ \varphi_2(\mathbf{x};t+2\tau) \end{pmatrix} = \begin{pmatrix} e^{-i[\hat{\mathbf{p}}^2/2m+V_1(\hat{\mathbf{x}})]\tau} & 0 \\ 0 & e^{-i[\hat{\mathbf{p}}^2/2m+V_2(\hat{\mathbf{x}})]\tau} \end{pmatrix} \times \begin{pmatrix} \varphi_1''(\mathbf{x};t+\tau) \\ \varphi_2''(\mathbf{x};t+\tau) \end{pmatrix}. \tag{9}$$

.

Step (III) can be combined with step (I) of the next propagation time slice for all but the last propagation time increment.

The diabatic propagation of individual wave-packet components [steps (I) and (III)] is based on the MP/SOFT implementation of the Trotter expansion,

$$e^{-i[\hat{\mathbf{p}}^2/2m+V_k(\hat{\mathbf{x}})]\tau} \approx e^{-iV_k(\hat{\mathbf{x}})\tau/2} e^{-i\hat{\mathbf{p}}^2/(2m)\tau} e^{-iV_k(\hat{\mathbf{x}})\tau/2}, \tag{10}$$

as described in Refs. 5 and 7. The underlying propagation scheme can be outlined as follows.

(1) Decompose the target functions $\varphi_l'(\mathbf{x};t) \equiv e^{-iV_l(\hat{\mathbf{x}})\tau/2}\varphi_l(\mathbf{x};t)$ into matching-pursuit coherent-state expansions,

$$\varphi_l'(\mathbf{x};t) \approx \sum_{j=1}^{n} c_j^{(l)} \langle \mathbf{x}|\chi_j\rangle. \tag{11}$$

Here, $\langle \mathbf{x}|\chi_j\rangle$ are $N$-dimensional coherent states,

$$\langle \mathbf{x}|\chi_j\rangle \equiv \prod_{k=1}^{N} A_j(k) \exp\left[ -\frac{\gamma_j(k)}{2}(x(k)-x_j(k))^2 + ip_j(k) \times (x(k)-x_j(k)) \right], \tag{12}$$

where $A_j(k)$ are normalization factors and $\gamma_j(k)$, $x_j(k)$, and $p_j(k)$ are complex-valued parameters selected according to the matching-pursuit algorithm, as described below. The expansion coefficients $c_j^{(l)}$, introduced by Eq. (11), are defined as follows: $c_1^{(l)} \equiv \langle \chi_1|\varphi_l'\rangle$ and $c_j^{(l)} \equiv \langle \chi_j|\varphi_l'\rangle - \Sigma_{k=1}^{j-1} c_k^{(l)} \langle \chi_j|\chi_k\rangle$ for $j=2-N$.

(2) Apply the kinetic energy part of the Trotter expansion to $\varphi_l'(\mathbf{x};t)$ by first Fourier transforming the coherent-state expansion of $\varphi_l'(\mathbf{x};t)$ to the momentum representation, multiplying it by $\exp[-i(\mathbf{p}^2/2m)\tau]$ and finally computing the inverse Fourier transform of the product to obtain

$$\varphi_l''(\mathbf{x};t) = \sum_{j=1}^{n} c_j^{(l)} \langle \mathbf{x}|\tilde{\chi}_j\rangle, \tag{13}$$

where

$$\langle \mathbf{x}|\tilde{\chi}_j\rangle \equiv \prod_{k=1}^{N} A_j(k) \sqrt{\frac{m}{m+i\tau\gamma_j(k)}} \times \exp\left( \frac{(p_j(k)/\gamma_j(k) - i[x_j(k)-x(k)])^2}{2/\gamma_j(k) + 2i\tau/m} - \frac{p_j(k)}{2\gamma_j(k)} \right). \tag{14}$$

The time-evolved wave-function components are thus

$$\varphi_l(\mathbf{x};t+\tau) = \sum_{j=1}^{n} c_j^{(l)} e^{-iV(\mathbf{x})\tau/2} \langle \mathbf{x}|\tilde{\chi}_j\rangle, \tag{15}$$

which can be reexpanded in coherent states as in step (1).

In the present study, step (II) can be performed analytically, since the wave-packet components $\varphi_1'$ and $\varphi_2'$ are represented as coherent-state expansions [see Eq. (11)] and the couplings $V_c(\mathbf{x})$ are expanded to second order accuracy in powers of $\mathbf{x}$ (see Sec. II C). Therefore, the underlying computational task necessary for nonadiabatic propagation is completely reduced to generating the coherent-state expansions defined by Eq. (11). In general, however, step (II) requires a matching-pursuit coherent-state reexpansion of the target states $\varphi_1''$ and $\varphi_2''$. As described in the Appendix, such a reexpansion can be efficiently combined with the diabatic propagation in order to avoid an extra computational overhead.

Coherent-state expansions are obtained by combining the matching-pursuit algorithm with a gradient-based optimization technique as follows.

(a) Starting from an initial trial coherent state $|\chi_j\rangle$, optimize the parameters $x_j(k)$, $p_j(k)$, and $\gamma_j(k)$ so that they locally maximize the overlap with the target state $|\varphi_l'(t)\rangle$. In the present study, initial guess parameters $\gamma_j(k)$, $x_j(k)$, and $p_j(k)$ are chosen as defined by the basis elements of previous wave-packet representation (or initial state) and they are locally optimized according to a steepest descent optimization procedure. The first basis function is the state $|\chi_1\rangle$ that locally maximizes the overlap with the target state,

$$|\varphi_l'(t)\rangle = c_1|\chi_1\rangle + |\epsilon_1\rangle, \tag{16}$$

where $c_1 \equiv \langle \chi_1|\varphi_l'(t)\rangle$ and $|\epsilon_1\rangle$ is the residual state after projecting out $|\chi_1\rangle$ from $|\varphi_l'(t)\rangle$. Note that $|\epsilon_1\rangle$ is or-

thogonal to $|\chi_1\rangle$, due to the definition of $c_1$. Therefore, $|\epsilon_1| \leqslant |\varphi_l'(t)|$.

(b) Subdecompose $|\epsilon_1\rangle$, analogously, as follows;

$$|\epsilon_1\rangle = c_2|\chi_2\rangle + |\epsilon_2\rangle, \tag{17}$$

where $c_2 \equiv \langle\chi_2|\epsilon_1\rangle$. Note that $|\epsilon_2| \leqslant |\epsilon_1|$, since $|\chi_2\rangle$ is orthogonal to $|\epsilon_1\rangle$.

Step (b) is repeated each time on the following residue. After $n$ successive orthogonal projections, the norm of the resulting residue $|\epsilon_n|$ is smaller than a desired precision $\varepsilon$,

$$|\epsilon_n| = \sqrt{1 - \sum_{j=1}^{n} c_j^2} \leqslant \varepsilon, \tag{18}$$

defining the truncation of the matching-pursuit expansion.

The resulting nonadiabatic propagation scheme is a natural generalization of the MP/SOFT method described in Ref. 5. In fact, in the limiting case of adiabatic quantum dynamics (i.e., $V_{jk}(\mathbf{x})=0$), the two methods are identical. The generalized MP/SOFT method also reduces to the perturbational approach introduced in Ref. 7 when the coupling matrix elements, introduced by Eq. (7), are expanded to first or second order accuracy in powers of the propagation time increment $\tau$. In contrast to such a perturbational scheme, however, the novel approach is rigorous and unitary.

### B. Calculation of photoabsorption spectra

The $S_2$ photoabsorption spectrum $I(\omega)$ is computed as the Fourier transform of the survival amplitude $C(t)$,

$$I(\omega) \propto \omega \int_{\infty}^{\infty} dt C(t) e^{i(\omega+\epsilon_0)t}, \tag{19}$$

where $\epsilon_0$ denotes the energy of the ground vibrational state of pyrazine and $\omega = 2\pi c/\lambda$. The time-dependent survival amplitude,

$$C(t) = \langle\Psi(0)|e^{-i\hat{H}t}|\Psi(0)\rangle = \int d\mathbf{x}\Psi^{\star}(\mathbf{x};-t/2)\Psi(\mathbf{x};t/2), \tag{20}$$

is obtained by overlapping the time-evolved states $\Psi(\mathbf{x};t/2) = e^{-i\hat{H}t/2}\Psi(\mathbf{x};0)$ and $\Psi(\mathbf{x};-t/2) = e^{i\hat{H}t/2}\Psi(\mathbf{x};0)$, after propagating the initial state $\Psi(\mathbf{x};0)$ forward and backward in time on the nonadiabatically coupled excited electronic states. Here, $\Psi(\mathbf{x};0)$ is the initial ground-state wave function multiplied by the transition dipole moment which is assumed to be constant as a function of nuclear coordinates (Condon approximation).

The initial state is defined according to Eq. (5) in terms of the two ground vibrational state wave-packet components,

$$\varphi_1(\mathbf{x};0) = 0,$$
$$\varphi_2(\mathbf{x};0) = \prod_{j=1}^{N} \left(\frac{1}{\pi}\right)^{1/4} e^{-x_j^2/2}, \tag{21}$$

associated with the $S_1$ and $S_2$ states, respectively. Here, $N$ is the dimensionality of the system, as defined by the number of vibrational modes explicitly considered in the model (i.e., $N=4$ in the reduced model system and $N=24$ in the full-dimensional model).

Earlier calculations have simulated the experimental broadening of the spectra, due to finite resolution of the spectrometer, by convoluting the photoabsorption spectra with a suitable experimental resolution function. In order to allow for direct comparisons with these earlier theoretical studies, the survival amplitude is damped with a single exponential,[12]

$$h(t) = \exp\left(-\frac{|t|}{\tau}\right), \tag{22}$$

leading to a Lorentzian broadening of the spectrum with full width at half maximum (FWHM) $\Gamma = 2/\tau$. The experimental broadening is reproduced by using $\tau = 150$ fs for the 24-dimensional model, and $\tau \approx 30$ fs for the reduced four-dimensional system. Furthermore, in order to reduce the effects of truncation due to the finite-time propagation, the calculated spectrum is convoluted with a sinc function which has a FWHM $= 2.5/T$, where $T = 150$ fs is the finite propagation time. The convolution is implemented by smoothly zeroing the survival amplitude at $t=T$ with the damping function[12]

$$g(t) = \cos\left(\frac{\pi t}{2T}\right). \tag{23}$$

### C. Model Hamiltonian

A detailed analysis of the model Hamiltonian, used for the reported MP/SOFT simulations, is readily available in Ref. 12. Here, the model is described only briefly.

The Hamiltonian, introduced by Eq. (2), is defined as follows:

$$\hat{H}_0 = \sum_j -\frac{1}{2m_j}\frac{\partial^2}{\partial Q_j^2}(|1\rangle\langle 1| + |2\rangle\langle 2|) + \sum_j \frac{1}{2} m_j \omega_j^2 Q_j^2 (|1\rangle \times \langle 1| + |2\rangle\langle 2|) + \Delta(|2\rangle\langle 2| - |1\rangle\langle 1|) + \sum_{i\in G_1} (a_i|1\rangle\langle 1| + b_i|2\rangle\langle 2|)Q_i + \sum_{(i,j)\in G_2} (a_{i,j}|1\rangle\langle 1| + b_{i,j}|2\rangle\langle 2|)Q_iQ_j \tag{24}$$

and

$$\hat{V}_c = \sum_{i\in G_3} c_i(|1\rangle\langle 2| + |2\rangle\langle 1|)Q_i + \sum_{(i,j)\in G_4} c_{i,j}(|1\rangle\langle 2| + |2\rangle \times \langle 1|)Q_iQ_j. \tag{25}$$

The parameters introduced by these equations have been obtained at the complete-active-space self-consistent-field (CASSCF) *ab initio* level,[18] including a total of 102 coupling constants $a_i$, $b_i$, $c_i$, $a_{i,j}$, $b_{i,j}$, and $c_{i,j}$, explicitly describing the 24 vibrational modes of pyrazine.[12] It is important to note that these parameters have been kindly supplied by Raab *et al.* and are slightly different from those reported in Ref. 12. In addition, to facilitate the comparison with experimental data, the 24-dimensional potential energy surfaces were shifted in energy by 4.06 eV.

The first and second terms, introduced by Eq. (24), define the harmonic expansion of the diabatic surfaces, where $\omega_j$ are the experimental ground-state vibrational frequencies and $m_j=\omega_j^{-1}$. Further, $Q_j=(x_j-x_j^{\mathrm{eq}})/(m_j\omega_j)^{-1/2}$ are the dimensionless normal-mode coordinates. The third term in Eq. (24) introduces the couplings between the $S_1$ and $S_2$ potential energy surfaces at the ground-state equilibrium configuration ($\mathbf{Q}=0$). The fourth and fifth terms in Eq. (24) include the linear and quadratic contributions to the diabatic-state expansions, where $G_1$ and $G_2$ indicate the set of modes having $A_g$ and $B_{2g}$ symmetries, respectively. The nonadiabatic couplings are described to second order accuracy, as given by Eq. (25), where $G_3$ represents the modes with symmetry $B_{1g}$ that linearly couple the $S_1$ and $S_2$ states and $G_4$ is the set of all pairs of modes the product of which has $B_{1g}$ symmetry, including the combinations $A_g\times B_{1g}$, $B_{2g}\times B_{3g}$, $A_u\times B_{1u}$, and $B_{2u}\times B_{3u}$.

The reduced four-mode model is constructed by following earlier work,[12] including only the vibronic coupling mode $\nu_{10a}$ and the three totally symmetric modes with the strongest linear coupling parameters, $\nu_{6a}$, $\nu_1$, and $\nu_{9a}$. In addition, to facilitate the comparison with experimental data, the four-dimensional potential energy surfaces were shifted in energy by 3.94 eV.

## III. RESULTS

This section demonstrates the capabilities of the generalized MP/SOFT method, introduced in Sec. II, as applied to the description of the ultrafast internal conversion of pyrazine at the $S_1/S_2$ conical intersection.

Figure 1 shows the comparison between the real and imaginary parts of the survival amplitude $C(t)=\langle\Psi_0|\Psi_t\rangle$, during the first 150 fs of dynamics, as predicted by the four-mode model Hamiltonian introduced in Sec. II C. Figure 1 also compares the MP/SOFT results (dots) with benchmark grid-based calculations (solid lines). MP/SOFT calculations are converged by using dynamically adaptive coherent-state expansions with $n=200$ basis functions. Grid-based SOFT calculations required representations on basis set of 1 048 576 grid points, defined in the range of normal mode coordinates $|Q_{10a}|\leqslant 7.0$ a.u., $|Q_{6a}|\leqslant 7.0$ a.u., $|Q_1|\leqslant 7.0$ a.u., and $|Q_{9a}|\leqslant 7.0$ a.u.. The integration time step was defined as $\tau=0.25$ fs for both grid-based and MP/SOFT calculations.

Figure 2 shows the photoabsorption spectra, obtained by Fourier transform of the survival amplitudes presented in Fig. 1, as described in Sec. II B. The efficiency of the MP/SOFT method is demonstrated in terms of the rather modest number of basis functions ($n=200$) required by the matching-pursuit coherent-state propagation, as compared to the rather demanding (memory/storage) requirements of the corresponding grid-based calculations (1 048 576 grid points).

The excellent agreement between MP/SOFT and benchmark grid-based calculations, during the whole dynamical range of $S_1/S_2$ internal conversion, demonstrates that the generalized MP/SOFT methodology introduced in this paper is a numerically exact and practical approach for the description of nonadiabaticity. The ultrafast falloff of the overlap between the initial and the time-evolved wave functions, within the first 15 fs of dynamics (Fig. 1), is caused by the wave packet moving away from its initial state and internal converting at the conical intersection between the $S_1$ and $S_2$ excited states. This ultrafast relaxation is responsible for the broad photoabsorption band in the frequency domain (Fig. 2). All the subsequent dynamics, at longer times, determines the diffuse structure superimposed to the broadband in the frequency domain. The longer time dynamics gives rise to a first recurrence feature at $t\approx 30$ fs (the subsequent at $t\approx 60$ fs, etc.) due to the partial recurrencies of the time-evolved wave function to the initial state. This phenomenon, which is common to other polyatomic systems where the

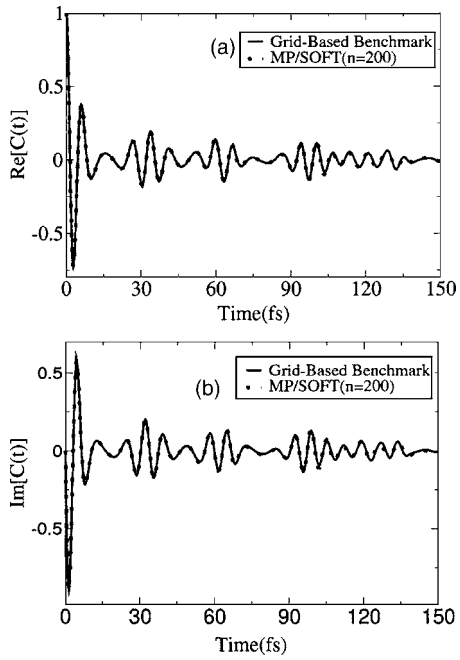


FIG. 1. Comparison between the real part (a) and the imaginary part (b) of the survival amplitude $C(t)=\langle\Psi_0|\Psi_t\rangle$, during the first 150 fs of dynamics after $S_0\rightarrow S_2$ photoexcitation of pyrazine, as predicted by the four-mode model Hamiltonian described in Sec. II C. The spectra are convoluted with a survival amplitude damping factor $\tau=30$ fs, as described in Sec. II B. MP/SOFT results (dots) are compared to benchmark grid-based calculations (solid lines).

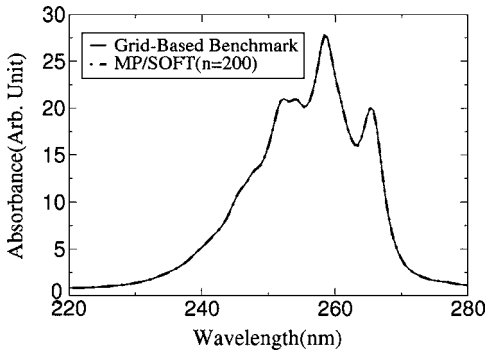


FIG. 2. Photoabsorption spectra of pyrazine predicted by the four-mode model Hamiltonian described in the text (Sec. II C). Benchmark quantum calculations (solid line) are compared to MP/SOFT results (dots) implemented as described in Sec. II A. Both spectra are convoluted with a survival amplitude damping factor $\tau=30$ fs, as described in Sec. II B.

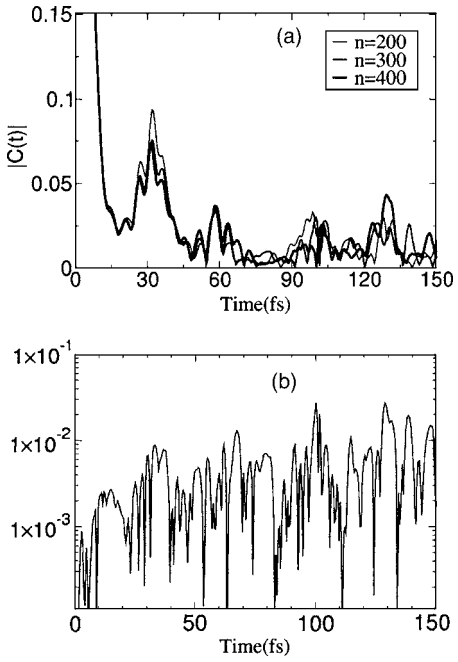


FIG. 3. (a) Comparison between the absolute values of $C(t)$, predicted by the MP/SOFT methodology during the first 150 fs of dynamics after $S_0 \rightarrow S_2$ photoexcitation of pyrazine, with $n=200$, 300, and 400 coherent-state basis functions. (b) Absolute value of survival amplitude differences obtained with $n=300$ and $n=400$, illustrating the convergence rate and the quality of the calculations.

potential energy surfaces responsible for excited-state relaxation are coupled at a conical intersection,[69] is quantitatively described by the MP/SOFT approach.

Figures 3 and 4, respectively, report the corresponding calculations of survival amplitudes and photoabsorption spectra for the 24-dimensional model of pyrazine. Figure 3, panel (a), shows the comparison of the absolute values of $C(t)$ as predicted by the MP/SOFT methodology with coherent-state expansions based on $n=200$, 300, and 400 coherent-state basis functions. Figure 3, panel (b), illustrates the convergence rate and the quality of the calculations by showing the absolute value of the differences between survival amplitudes obtained with $n=300$ and $n=400$. It is shown that the differences in $C(t)$ obtained by increasing the number of basis functions in the model oscillate, reaching a

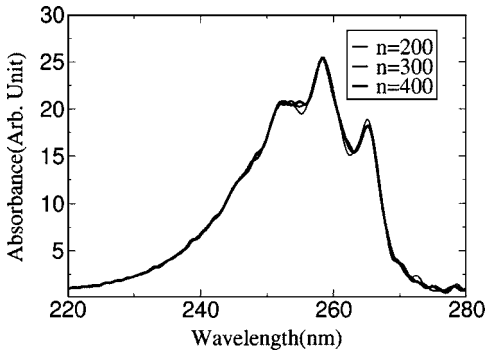


FIG. 4. Comparison between the pyrazine photoabsorption spectra obtained by implementing the MP/SOFT methodology with $n=200$, 300, and 400 coherent-state basis functions. The spectra are convoluted with a survival amplitude damping factor $\tau=150$ fs, as described in Sec. II B.

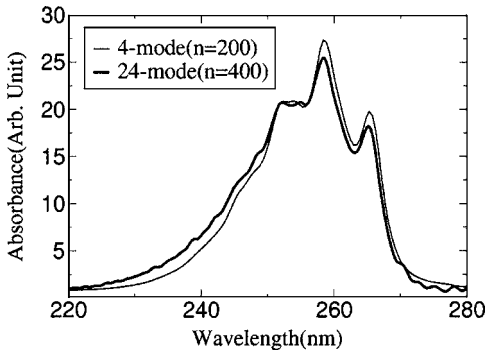


FIG. 5. Comparison between the photoabsorption spectra of pyrazine predicted by the 24-mode model ($\tau \approx 150$ fs, $n=400$) and the four-mode model ($\tau \approx 30$ fs, $n=200$) described in the text.

plateau of maximum values at about 100 fs. The resulting changes in the spectrum, arising from these differences, are shown in Fig. 4.

The comparison of the spectra and survival amplitudes, obtained with an increasing number of coherent states, indicates that the calculations scale only modestly with the dimensionality of the problem. In fact, even calculations based on 200 basis functions for the 24-dimensional model provide a very good approximation to fully converged results. These results favorably compare to the corresponding results obtained with state-of-the-art time-dependent methods, including MCTDH calculations based on 2 771 440 configurations and 502 200 configurations.[12]

Regarding computational expense, computations of survival amplitudes for 150 fs required 620 propagation steps. Both four-dimensional and 24-dimensional calculations, based on $n=200$ coherent states, were completed within 24 h on a parallel computer with 48 Opteron processors. Each processor runs at a clock speed of 2.2 GHz. Analogous calculations for the 24-dimensional model with $n=300$ and $n=400$ basis functions required 80 and 160 h, respectively, on the same parallel computer.

For completeness, Fig. 5 shows the calculated photoabsorption spectra, obtained for the four-mode model ($\tau \approx 30$ fs, $n=200$) as compared to the photoabsorption of the 24-mode model ($\tau \approx 150$ fs, $n=400$). This comparison indicates that, in the full-dimensional model, the remaining 20 vibrational modes influence the underlying spectroscopy of the reduced four-mode model similarly to the effect of a phenomenological broadening.

## IV. CONCLUDING REMARKS

We have introduced a numerically exact (nonperturbative) approach for simulations of nonadiabatic quantum dynamics. The resulting approach is a generalization of the recently developed MP/SOFT algorithm.[3–8] It is based on the recursive application of the time-evolution operator, as defined by the Trotter expansion to second order accuracy, in dynamically adaptive coherent-state expansions generated with the matching-pursuit algorithm. The coherent-state representations allow for an *analytic* evaluation of the Trotter expansion, bypassing the exponential scaling problem of the grid-based SOFT method. The resulting approach is unitary

and rigorous and becomes identical to the original MP/SOFT formulation[5] in the adiabatic limit (i.e., when the couplings are negligible). In addition, the method can be reduced to the recently developed perturbational scheme for simulations of nonadiabatic dynamics,[7] simply by expanding the coupling propagation matrix elements to first or second order accuracy in the propagation time increment.

We have demonstrated how to apply the generalized MP/SOFT method for computations of survival amplitudes and photoabsorption spectra of pyrazine, as described by a four-mode model Hamiltonian that allows for direct comparisons to benchmark grid-based calculations and a 24-mode model that describes the nonadiabatic dynamics at the $S_1/S_2$ conical intersection in full dimensionality. The reported computational results demonstrate that the MP/SOFT method is a practical and accurate approach to model nonadiabatic reaction dynamics in polyatomic systems, since both the accuracy and efficiency compare quite favorably with state-of-the-art time-dependent methods.

## ACKNOWLEDGMENTS

One of the authors (V.S.B.) acknowledges a generous allocation of supercomputer time from the National Energy Research Scientific Computing (NERSC) center and financial support from Research Corporation, Research Innovation Award No. RI0702, a Petroleum Research Fund Award from the American Chemical Society PRF No. 37789-G6, a junior faculty award from the F. Warren Hellman Family, the National Science Foundation (NSF) Career Program Award CHE No. 0345984, the NSF Nanoscale Exploratory Research (NER) Award ECS No. 0404191, the Alfred P. Sloan Fellowship (2005-2006), a Camille Dreyfus Teacher-Scholar Award for 2005, and a Yale Junior Faculty Fellowship in the Natural Sciences (2005-2006).

## APPENDIX: NONADIABATIC MP/SOFT

This section introduces the implementation of the MP/SOFT approach for simulations of nonadiabatic quantum dynamics, according to a propagation scheme where both the diabatic propagation and the mixing of wave-packet components are combined in a single matching-pursuit reexpansion procedure. The advantage of this alternative approach, relative to the method introduced in Sec. II, is that a single matching-pursuit reexpansion is required per propagation step, even for problems where the coupling of wave-packet components cannot be performed analytically.

The approach is based on the embedded form of the Trotter expansion,

$$e^{-i\hat{H}2\tau} \approx e^{-i(\hat{p}^2/2m)\tau} e^{-i\hat{V}_0(\mathbf{x})\tau} e^{-i\hat{V}_c(\mathbf{x})2\tau} e^{-i\hat{V}_0(\mathbf{x})\tau} e^{-i(\hat{p}^2/2m)\tau}, \tag{A1}$$

where $\hat{H}=\hat{p}^2/(2m)+\hat{V}_0+\hat{V}_c$, with $\hat{V}_0=V_1(\mathbf{x})|1\rangle\langle 1|+V_2(\mathbf{x})|2\rangle\times\langle 2|$ and $\hat{V}_c=V_c(\mathbf{x})|1\rangle\langle 2|+V_c(\mathbf{x})|2\rangle\langle 1|$.

The MP/SOFT implementation of Eq. (A1), as applied to the propagation of the initial state introduced by Eq. (5), involves the following steps.

(I) Analytically propagate $\varphi_1(\mathbf{x};t)$ and $\varphi_2(\mathbf{x};t)$ for time $\tau$, according to the free-particle propagator,

$$\begin{pmatrix} \varphi_1'(\mathbf{x};t+\tau) \\ \varphi_2'(\mathbf{x};t+\tau) \end{pmatrix} = \begin{pmatrix} e^{-i(\hat{\mathbf{p}}^2/2m)\tau} & 0 \\ 0 & e^{-i(\hat{\mathbf{p}}^2/2m)\tau} \end{pmatrix} \begin{pmatrix} \varphi_1(\mathbf{x};t) \\ \varphi_2(\mathbf{x};t) \end{pmatrix}. \tag{A2}$$

(II) Couple the two wave-packet components $\varphi_1'(\mathbf{x};t+\tau)$ and $\varphi_2'(\mathbf{x};t+\tau)$

$$\begin{pmatrix} \varphi_1''(\mathbf{x};t+\tau) \\ \varphi_2''(\mathbf{x};t+\tau) \end{pmatrix} = \mathbf{M} \begin{pmatrix} \varphi_1'(\mathbf{x};t+\tau) \\ \varphi_2'(\mathbf{x};t+\tau) \end{pmatrix}, \tag{A3}$$

with

$$\mathbf{M} \equiv \begin{pmatrix} \cos(2V_c(\hat{\mathbf{x}})\tau)e^{-i\hat{V}_1(\hat{\mathbf{x}})2\tau} & -i\sin(2V_c(\hat{\mathbf{x}})\tau)e^{-i(\hat{V}_1(\hat{\mathbf{x}})+\hat{V}_2(\hat{\mathbf{x}}))\tau} \\ -i\sin(2V_c(\hat{\mathbf{x}})\tau)e^{-i(\hat{V}_1(\hat{\mathbf{x}})+\hat{V}_2(\hat{\mathbf{x}}))\tau} & \cos(2V_c(\hat{\mathbf{x}})\tau)e^{-i\hat{V}_2(\hat{\mathbf{x}})2\tau} \end{pmatrix}. \tag{A4}$$

(III) Analytically propagate $\varphi_1''(\mathbf{x};t+\tau)$ and $\varphi_2''(\mathbf{x};t+\tau)$ for time $\tau$, according to the free-particle propagator,

$$\begin{pmatrix} \varphi_1(\mathbf{x};t+2\tau) \\ \varphi_2(\mathbf{x};t+2\tau) \end{pmatrix} = \begin{pmatrix} e^{-i(\hat{\mathbf{p}}^2/2m)\tau} & 0 \\ 0 & e^{-i(\hat{\mathbf{p}}^2/2m)\tau} \end{pmatrix} \times \begin{pmatrix} \varphi_1''(\mathbf{x};t+\tau) \\ \varphi_2''(\mathbf{x};t+\tau) \end{pmatrix}. \tag{A5}$$

In practice, however, step (III) is combined with step (I) of the next propagation time slice for all but the last propagation time increment.

Note that Eq. (A3) results, in analogy to Eq. (7), from considering that

$$e^{-i\mathbf{V}_c 2\tau} = \mathbf{D}^\dagger \begin{pmatrix} e^{iV_c(\mathbf{x})2\tau} & 0 \\ 0 & e^{-iV_c(\mathbf{x})2\tau} \end{pmatrix} \mathbf{D}, \tag{A6}$$

with

$$\mathbf{D} = \mathbf{D}^\dagger \equiv \begin{pmatrix} -1/\sqrt{2} & 1/\sqrt{2} \\ 1/\sqrt{2} & 1/\sqrt{2} \end{pmatrix}, \tag{A7}$$

since

$$e^{-i\mathbf{V}_c 2\tau} = \mathbf{1} + (-i\mathbf{V}_c 2\tau) + \frac{1}{2!}(-i\mathbf{V}_c 2\tau)^2 + \cdots \tag{A8}$$

and

$$\mathbf{V}_c \equiv \begin{pmatrix} 0 & V_c(\mathbf{x}) \\ V_c(\mathbf{x}) & 0 \end{pmatrix} = \mathbf{D}^\dagger \begin{pmatrix} -V_c(\mathbf{x}) & 0 \\ 0 & V_c(\mathbf{x}) \end{pmatrix} \mathbf{D}, \qquad \text{(A9)}$$

with $\mathbf{D}\mathbf{D}^\dagger = 1$.


[1] H. Nakamura, *Nonadiabatic Transitions: Concepts, Basic Theories, and Applications* (World Scientific, Singapore, 2002).
[2] A. Kondorskiy and H. Nakamura, J. Chem. Phys. **120**, 8937 (2004).
[3] Y. Wu and V. S. Batista, J. Chem. Phys. **118**, 6720 (2003).
[4] Y. Wu and V. S. Batista, J. Chem. Phys. **119**, 7606 (2003).
[5] Y. Wu and V. S. Batista, J. Chem. Phys. **121**, 1676 (2004).
[6] X. Chen, Y. Wu, and V. S. Batista, J. Chem. Phys. **122**, 64102 (2005).
[7] Y. Wu, M. F. Herman, and V. S. Batista, J. Chem. Phys. **122**, 114114 (2005).
[8] Y. Wu and V. S. Batista, J. Chem. Phys. **124**, 224305 (2006).
[9] I. Yamazaki, T. Murao, T. Yamanaka, and K. Yoshihara, Faraday Discuss. Chem. Soc. **75**, 395 (1983).
[10] K. K. Innes, I. G. Ross, and W. R. Moonaw, J. Mol. Spectrosc. **32**, 492 (1988).
[11] H. Köppel, W. Domcke, and L. S. Cederbaum, Adv. Chem. Phys. **57**, 59 (1984).
[12] A. Raab, G. A. Worth, H. D. Meyer, and L. S. Cederbaum, J. Chem. Phys. **110**, 936 (1999).
[13] G. Stock, C. Woywood, W. Domcke, T. Swinney, and B. S. Hudson, J. Chem. Phys. **103**, 6851 (1995).
[14] M. Thoss, W. H. Miller, and G. Stock, J. Chem. Phys. **112**, 10282 (2000).
[15] M. Ben-Nun and T. J. Martinez, Adv. Chem. Phys. **121**, 439 (2002).
[16] C. Coletti and G. D. Billing, Chem. Phys. Lett. **368**, 289 (2003).
[17] D. V. Shalashilin and M. S. Child, J. Chem. Phys. **121**, 3563 (2004).
[18] C. Woywood, W. Domcke, A. L. Sobolewski, and H. J. Werner, J. Chem. Phys. **100**, 1400 (1994).
[19] D. Neuhauser, J. Chem. Phys. **100**, 9272 (1994).
[20] W. Zhu, J. Z. H. Zhang, and D. H. Zhang, Chem. Phys. Lett. **292**, 46 (1998).
[21] G. C. Schatz, M. S. Fitzcharles, and L. B. Harding, Faraday Discuss. Chem. Soc. **84**, 359 (1987).
[22] D. C. Clary, J. Phys. Chem. **98**, 10678 (1994).
[23] R. Kosloff, Annu. Rev. Phys. Chem. **45**, 145 (1994).
[24] J. R. Fair, D. Schaefer, R. Kosloff, and D. J. Nesbitt, J. Chem. Phys. **116**, 1406 (2002).
[25] J. Echave and D. C. Clary, J. Chem. Phys. **100**, 402 (1994).
[26] H. G. Yu and J. T. Muckerman, J. Chem. Phys. **117**, 11139 (2002).
[27] M. I. Hernandez and D. C. Clary, J. Chem. Phys. **101**, 2779 (1994).
[28] D. Charlo and D. C. Clary, J. Chem. Phys. **117**, 1660 (2002).
[29] J. M. Bowman, J. Phys. Chem. A **102**, 3006 (1998).
[30] D. Q. Xie, R. Q. Chen, and H. Guo, J. Chem. Phys. **112**, 5263 (2000).
[31] S. M. Anderson, T. J. Park, and D. Neuhauser, Phys. Chem. Chem. Phys. **1**, 1343 (1999).
[32] M. D. Feit, J. A. Fleck, Jr., and A. Steiger, J. Comput. Phys. **47**, 412 (1982).
[33] M. D. Feit, J. A. Fleck, Jr., and A. Steiger, J. Chem. Phys. **78**, 301 (1983).
[34] D. Kosloff and R. Kosloff, J. Comput. Phys. **52**, 35 (1983).
[35] H. Tal-Ezer and R. Kosloff, J. Chem. Phys. **81**, 3967 (1984).
[36] T. J. Park and J. C. Light, J. Chem. Phys. **85**, 5870 (1986).
[37] R. K. Preston and J. C. Tully, J. Chem. Phys. **54**, 4297 (1971).
[38] J. C. Tully, J. Chem. Phys. **93**, 1061 (1990).
[39] R. B. Gerber, V. Buch, and M. A. Ratner, J. Chem. Phys. **77**, 3022 (1982).
[40] H. D. Meyer and W. H. Miller, J. Chem. Phys. **70**, 3214 (1979).
[41] X. Sun and W. H. Miller, J. Chem. Phys. **106**, 6346 (1997).
[42] M. Thoss and G. Stock, Phys. Rev. A **59**, 64 (1999).
[43] M. F. Herman and E. Kluk, Chem. Phys. **91**, 27 (1984).
[44] E. Kluk, M. F. Herman, and H. L. Davis, J. Chem. Phys. **84**, 326 (1986).
[45] G. Yang and M. F. Herman, J. Phys. Chem. B **105**, 6562 (2001).
[46] F. Webster, P. J. Rossky, and R. A. Friesner, Comput. Phys. Commun. **63**, 494 (1991).
[47] O. V. Prezhdo and P. J. Rossky, J. Chem. Phys. **107**, 825 (1997).
[48] D. F. Coker, in *Computer Simulation in Chemical Physics*, edited by M. P. Allen and D. J. Tildesley (Kluwer Academic, Dordrecht 1993), pp. 315–377.
[49] S. Hammes-Schiffer, J. Chem. Phys. **105**, 2236 (1996).
[50] S. Hammes-Schiffer and J. C. Tully, J. Chem. Phys. **103**, 8528 (1995).
[51] N. Makri and W. H. Miller, J. Chem. Phys. **91**, 4026 (1989).
[52] S. G. Mallat and Z. F. Zhang, IEEE Trans. Signal Process. **41**, 3397 (1993).
[53] W. H. Press, B. P. Flannery, S. A. Teukolsky, and W. T. Vetterling, *Numerical Recipes* (Cambridge University Press, Cambridge, 1986), Chap. 12.
[54] E. J. Heller, Chem. Phys. Lett. **34**, 321 (1975).
[55] M. J. Davis and E. J. Heller, J. Chem. Phys. **71**, 3383 (1979).
[56] E. J. Heller, J. Chem. Phys. **75**, 2923 (1981).
[57] R. D. Coalson and M. Karplus, Chem. Phys. Lett. **90**, 301 (1982).
[58] S. I. Sawada, R. Heather, B. Jackson, and H. Metiu, Chem. Phys. Lett. **83**, 3009 (1985).
[59] K. G. Kay, J. Chem. Phys. **91**, 107 (1989).
[60] M. Ben-Nun and T. J. Martinez, J. Chem. Phys. **108**, 7244 (1998).
[61] K. Thompson and T. J. Martinez, J. Chem. Phys. **110**, 1376 (1999).
[62] J. D. Coe and T. J. Martinez, J. Am. Chem. Soc. **127**, 4560 (2005).
[63] J. D. Coe and T. J. Martinez, J. Phys. Chem. A **110**, 618 (2006).
[64] D. V. Shalashilin and B. Jackson, Chem. Phys. Lett. **291**, 143 (1998).
[65] L. M. Andersson, J. Chem. Phys. **115**, 1158 (2001).
[66] D. V. Shalashilin and M. S. Child, J. Chem. Phys. **113**, 10028 (2000).
[67] D. V. Shalashilin and M. S. Child, J. Chem. Phys. **115**, 5367 (2001).
[68] M. H. Beck, A. Jackle, G. A. Worth, and H. D. Meyer, Phys. Rep. **324**, 1 (2000).
[69] V. S. Batista and W. H. Miller, J. Chem. Phys. **108**, 498 (1998).